THE SUPERCONDUCTING 130 MeV ELECTRON ACCELERATOR AT DARMSTADT *)

V. Aab, K. Alrutz-Ziemssen, R. Amend, D. Flasche, H.-D. Gräf, V. Huck, K. D. Hummel, M. Knirsch, F. Lindqvist, W. Lotz, A. Richter, T. Rietdorf, U. Schaaf, S. Simrock, E. Spamer, O. Titze, H. Weise, W. Ziegler
Institut für Kernphysik, Technische Hochschule Darmstadt, Schlossgartenstr. 9, D-6100 Darmstadt, Germany

and

H. Heinrichs, H. Piel, J. Pouryamout
Fachbereich Physik, Universität Gesamthochschule Wuppertal, Gauss-Str. 20, D-5600 Wuppertal, Germany

I. Introduction

We report here on a 130 MeV superconducting cw electron accelerator presently under construction. This accelerator results from a cooperative effort between the Physics Department of the Universität Gesamthochschule Wuppertal and the Technische Hochschule Darmstadt. The accelerator henceforth called recyclotron for reasons which will become clear below is being installed at the Nuclear Physics Institute at Darmstadt. It will replace the existing [1] low duty factor ($< 10^{-3}$) 70 MeV linear accelerator DALINAC which is in operation since 1962 and is still used for single arm high resolution electron scattering experiments. The new accelerator because of its cw beam will allow for coincidence measurements giving a much more detailed insight into nuclear structure as determined from inclusive inelastic electron scattering.

The choice of a superconducting accelerator and its basic design parameters have been discussed earlier [2] and a first status report [3] has been given about one year ago. Therefore in Sect. II we give only a short summary of the parameters finally chosen whereas the present status of the construction is presented more in detail. In Sect. III the development of the rf control circuits which took most of our efforts last year is described. Results from the first successful operation of the superconducting injector linac are presented in Sect. IV, while Sect.V contains a short outlook how we intend to complete the construction of the accelerator and on future developments.

II. Present Status

The general layout of the 130 MeV recyclotron is shown in Fig. 1. A dc electron beam produced by the electron gun (1) is electrostatically preaccelerated to a kinetic energy of 250 keV. After passing a chopper and prebuncher section the beam enters the superconducting injector linac (2) and is accelerated to 10 MeV. An isochronous 180^{o} deflection system takes it to the superconducting main linac (3) where it gains another 40 MeV. Two beam transport systems (4), (5) each one consisting of two isochronous 180^{o} bends and a straight section allow to recirculate the beam another two times through the main linac, yielding a maximum energy of 130 MeV. Then the beam is transported to the existing experimental facilities (to the right of Fig. 1 and not shown there). In the straight beamline behind the 10 MeV injector two experimental setups, indicated by a dashed line in Fig. 1, a channeling radiation source and a bremsstrahlung facility for nuclear resonance fluorescence investigations have been installed.

*) Work supported by Deutsche Forschungsgemeinschaft

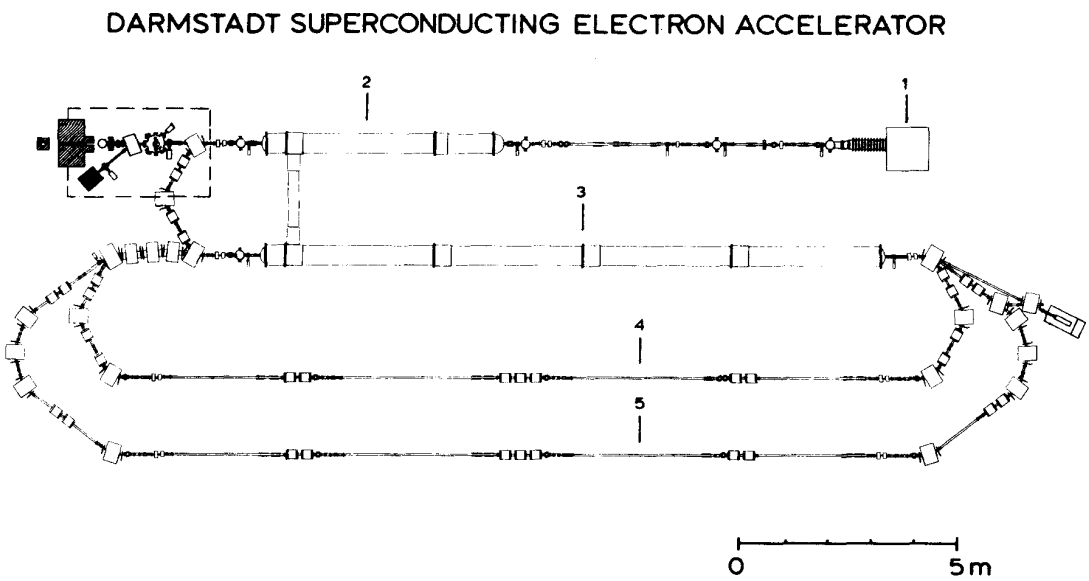

Fig. 1 **Schematic layout of the superconducting 130 MeV recyclotron**

The main design parameters of the superconducting accelerator are given in Tab. 1 below.

Table 1: Design parameters of the 130 MeV superconducting electron accelerator

General	Beam energy (MeV)	10 - 130
	Energy spread (keV)	± 13
	cw current (μA)	≥ 20
Accelerating structure	Type	standing wave
	Mode	π
	Frequency (MHz)	2997
	Operating temperature (K)	2
	Quality factor	$3 \cdot 10^9$
	Accelerating field (MV/m)	5
	Power dissipation (W)	4
	Number of structures 1.00 m long	10
	Capture section 0.25 m long	1

In the following the present status of the various sections of the recyclotron is given in turn.

Room temperature injection

It consists of the electron gun, an electrostatic preaccelerator tube, rf chopper- and prebuncher cavities, two magnetic lenses, horizontal and vertical steerers, three viewscreens, two wirescanners and an rf beam intensity- and position monitor. The electron gun which delivers a dc current of $i < 2$ mA is mounted together with the associated power supplies and control electronics

inside a high voltage terminal. Control of filament, beam intensity and two steering coils which had to be incorporated into the gun is achieved via a serial data link, consisting of two 25 m long fibre optics. The preacceleration voltage of 250 kV is generated by a 300 kV/5 mA power supply with a short- and long term stability of $< \pm 10^{-4}$. The acceleration tube is a 34 stage metal-glass construction without O-ring seals.

The chopper section consists of one cylindrical cavity in which both orthogonal TM_{110}-like modes are excited and a watercooled copper orifice with a 2 mm bore 2 m downstream the beamline. The dc beam from the gun is chopped into segments corresponding to 30 degrees of rf phase. A standard prebuncher cavity follows the chopper section and compresses the preformed 30 degree bunch to 6 degrees at the position where it enters the capture section of the superconducting injection linac.

This part of the accelerator has been operated routinely over the last year and has proved to work satisfactorily. The emittance of the 250 keV beam has been measured to be 0.2 π mm mrad in the vertical and 0.4 π mm mrad in the horizontal direction, well below the design acceptance of the superconducting injector linac, which is 1.8 π mm mrad. After the installation of a set of Helmholtz coils for compensation of the earthmagnetic field almost no additional steering corrections are needed in this section.

Cryogenics

As indicated in Fig. 1 the cryostats for the injector and main linac consist of 5 identical modules each 3.4 m long, 1 short module (1.4 m long), 4 end caps and an element connecting the two cryostats. The short module contains the 5 cell capture section whereas each of the long modules takes two 20 cell accelerating structures.

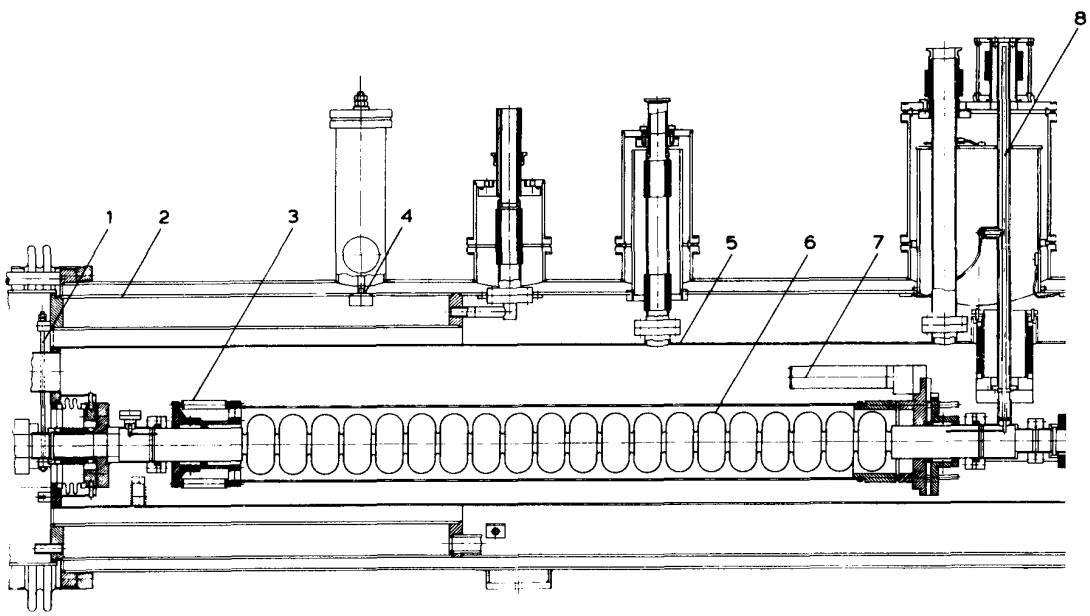

Fig. 2 Cross section of one half of a cryomodule with accelerating structure

A cross section of one half of such a module is shown in Fig. 2. The superconducting structure (6) with its tuning frame, motor driven coarse tuner (7) and piezoelectric translators (3) for fine tuning is mounted in an aluminum bench (not shown in Fig. 2) inside the helium tank (5). It is carried by 4 stainless steel tubes (1), connected to the liquid nitrogen cooled radiation shield (2). The shield itself is connected (4) to the outer vacuum jacket of the cryostat also by stainless steel tubes, adjustable from the outside. The rf input consists of a 7/8" coaxial line. Its center conductor is formed by a thin wall copper tube, whereas the outer conductor is fabricated from stainless steel, copperplated on the inside. Most of the heatflow is directed via a $\lambda/4$ shorting stub to the radiation shield at liquid nitrogen temperature. Two ceramic windows, one at room temperature, one at 2 K, are incorporated in this input line.

The present configuration consists of the injector cryostat, fully equipped with a capture section and two 20 cell structures, one module of the main linac without accelerating structures and the connecting element. Standby losses at 2 K amount to slightly less than 10 W. The refrigerator has a power of 100 W at 2 K. It has been in operation for several periods of many weeks during the last year and it works very satisfactorily but some shortcomings of the four stage roots pump, necessary for the 2 K operation, have still prevented a power and final acceptance test.

Beam transport system

For the injection, the two recirculations and the extraction a total of 22 dipole magnets and 34 quadrupoles have been installed. A collection of the magnet data is given in Tab. 2 below.

Table 2: Properties of the dipole and quadrupole magnets

Dipole magnets	Number	22
	Induction (T)	≤ 0.7
	Power consumption (kW)	≤ 1.9
	Gap (mm)	30
	Weight (t)	0.27
Quadrupole magnets	Number	34
	Effective length (mm)	194.3
	Gradient (T/m)	≤ 6.5
	Power consumption (W)	≤ 80
	Aperture (mm)	40
	Weight (t)	0.055

The isochronous 180^{o} bends of the injection and the first recirculation are of the well known design using 3 dipoles and 4 quadrupoles (see Fig. 1), whereas in the bends of the second recirculation the central dipole has been split up into three magnets. The straight sections of the recirculations contain two quadrupole doublets and one triplet each. Proper reinjection of the beam into the main linac is achieved by a chicane, using three additional dipoles. The beam is extracted either directly from the splitting magnet behind the main linac or from an extraction magnet in the second recirculation. For diagnostics combinations of rf intensity and position monitors are used at each end of the two cryostats and the straight sections of the recirculations. Viewscreens have been positioned in the beamline where according to the beam optics calculations a waist of the beam is expected. The photograph in Fig. 3 shows the accelerator as seen from the extraction side and gives an impression of the present status.

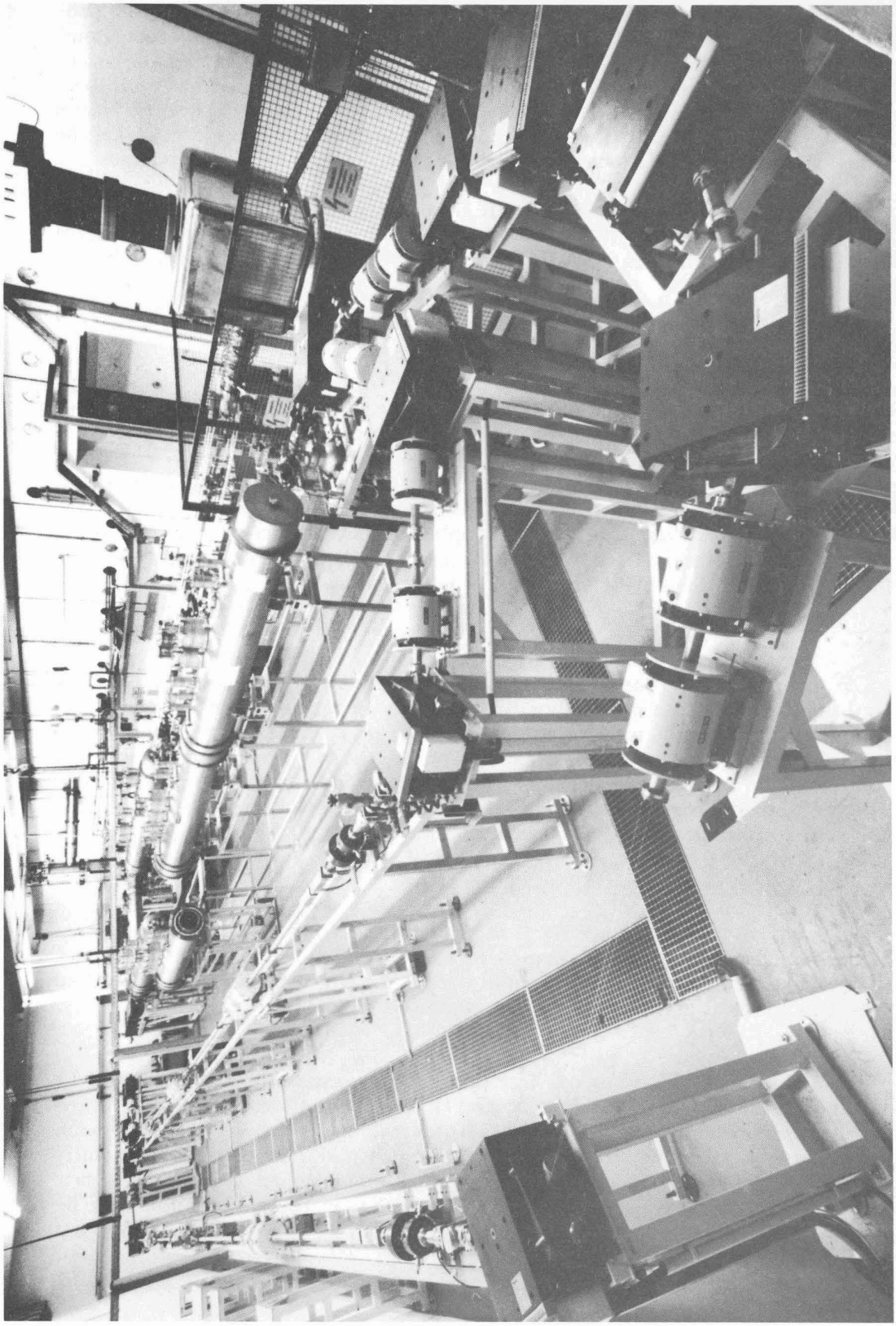

Fig. 3 View of the accelerator as seen from the extraction side

Computer Control

The recyclotron will be operated with 2 minicomputers (DEC LSI 11/73) interconnected by DECnet/Ethernet. One system located in the local control area handles all machine control interfaces. All process parameters collected here in a central parameter data base are handled by one process control program. All other utilities necessary for machine control like operator input, status information, parameter display, set up save/restore facilities interface uniquely to this control program. This includes also remote access via local area network necessary for a second LSI 11/73 located in the new control room in another part of the building. Both minicomputer systems have access to the laboratory VAX 11/750 for extended calculations and program development.

The local system is operational, all Ethernet connections are set up, the integration of the remote LSI 11/73 (main control room) into the process control system will be completed as soon as the interior of the new control room is finished.

RF Transmitters

Twelve individual rf channels are provided, one for each of the 20 cell accelerating structures, one for the capture section and one for the chopper and prebuncher resonators. As power amplifiers watercooled klystrons type TH 2047W (5 kV/0.5 A) delivering ≥ 500 W of rf power each are used. Reflected power from the superconducting structures is absorbed in watercooled isolators. As transmission lines standard air filled 7/8" coaxial lines were chosen. For monitoring purposes a dual directional coupler of high directivity (≥ 45 dB) is used in each line before it enters the cryostate. The control circuits will be described in detail in Sect. III below.

III. RF Control Circuits

The properties of the superconducting accelerating structures as they are mounted in their tuning frames inside the cryostate together with the environmental conditions (pressure oscillations, mechanical vibrations, etc.) determine by which way and how well a phase locked operation of several structures can be achieved. Therefore this section describes in detail these properties obtained from a series of rf tests and the solution for the low power rf control circuits finally chosen.

Properties of the superconducting structures

The way the structures are fixed in their tuning frames and how mechanical coarse and fine tuning is performed is shown in Fig. 4. The 5 cell capture section has been chosen as an example because here details can be studied best. The 1 m long 20 cell structures are mounted exactly the same way.

The niobium cutoff tubes on both sides of the structure (3) are held by solid brass flanges. The motor driven coarse tuner (2) uses 3 axles with differential threads synchronously driven to obtain a total change in length of 2 mm. The structure is surrounded by a titanium tube (6) and supported horizontally and vertically at every second cell. Fine tuning is accomplished by 3 piezoelectric translators (4) giving a length change of 40 μm/1 kV at room temperature. The left part of Fig. 4 shows the rf input coupler (1) with its ceramic window and

niobium antenna. On the right side the end of the output coupler antenna (5) is indicated.

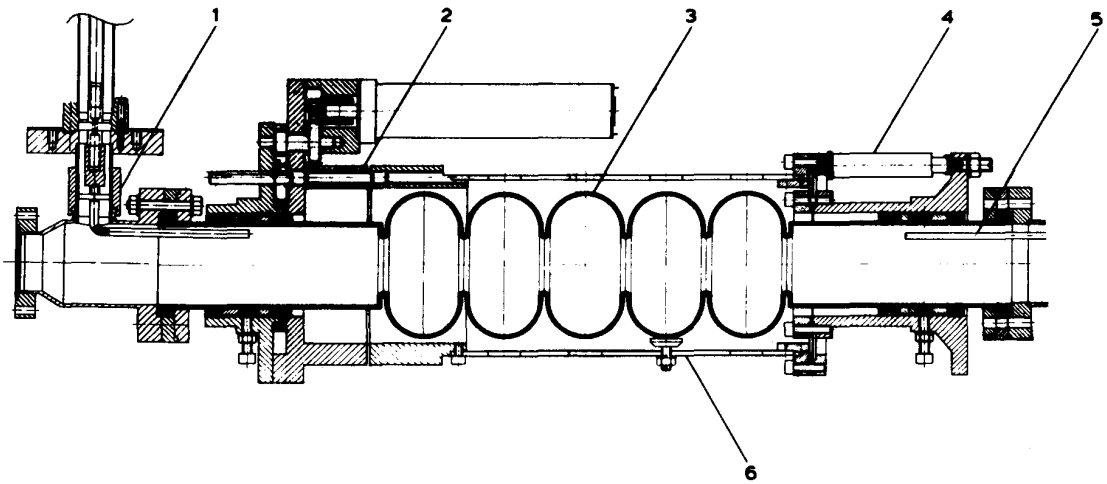

Fig. 4 Five cell capture section with couplers and tuners

Already a first rf test at 2 K [3] showed that the original concept of dynamically fine tuning the structures (with frequencies of up to a few hundred Hz) could not be realized. The reason is that the structures show a group of strong mechanical resonances between 300 and 400 Hz, which cause the feedback control circuit of the piezoelectric translators to become unstable. In late Summer 86 the injector linac was equipped with a new set of accelerating structures (the ones used in the first test had suffered too much from a long exposure to air). Simultaneously investigations and a series of rf tests at 2 and 4 K were performed to find out what caused the phase instabilities and how they could be avoided or controlled. Table 3 gives a collection of some results from these measurements combined with the typical rf properties of the superconducting structures.

Table 3: Typical sensitivities of a 20 cell structure at 3 GHz

Tuning range	Coarse tuner (MHz)	1.2
	Fine tuner (kHz)	0.3
Variations in	Length (kHz/mm)	500
	Pressure (Hz/mbar)	≈ 15

Recalling that the stability requirements for the accelerating field strength and the rf phase are $\Delta E/E \leq 10^{-4}$ and $\Delta\Phi < 1^{\circ}$ respectively according to the design parameters of the accelerator (see Tab. 1) one can derive a phase sensitivity $\Delta\Phi$ to changes in the resonant frequency $\Delta\nu_0$ of

$$\Delta\Phi/\Delta\nu_0 \approx (Q_L/Q_0) \cdot 90^{\circ}/\mathrm{Hz}.$$

Since the attempted ratio Q_L/Q_0 is 0.01 (at present it is about 0.05) with $Q_0 \approx 3 \cdot 10^9$ at 3 GHz the phase sensitivity to changes in length of the 1 m long

structure or in pressure will be $\Delta\Phi/\Delta L \approx 2\ ^{o}/nm$ and $\Delta\Phi/\Delta p \approx 15\ ^{o}/mbar$, respectively, if the structure is driven at a fixed frequency.

The rf tests mentioned above showed clearly that at 2 K the observed phase deviations between two structures were not caused by pressure oscillations. This is not true for 4 K operation when the roots pump is bypassed and a direct connection exists between the cryostat and the compressor suction side through the low pressure heat exchangers of the refrigerator. At 2 K, however, the distortions are due to vibrations generated by the refrigerator and coupled to the cryostat by the helium transfer line. An attempt to improve the situation by incorporating two bellows into the suction and pressure pipes between the compressor and the cold box has not been fully successful.

Since the design of the accelerating structures does not allow for an additional strong rf coupling as it would be necessary for phase control via an external voltage controlled reactance (VCX) we decided to achieve phase control by driving the structures with an rf input modulated in a special way which has proven to be successful in superconducting heavy ion accelerators [4,5]. Using a phase control circuit very similar to the one described in ref. [5] a phase locked operation of two 20 cell structures could be obtained for the first time in spring this year. The 5 cell capture section, however, showed much larger variations in its resonant frequency than the 20 cell structures. A double slug tuner had to be used in the rf input line to reduce the external Q to $Q_{ex} \approx 5 \cdot 10^{6}$ before a phase locked operation was possible and a beam could be accelerated in May 87 by two structures.

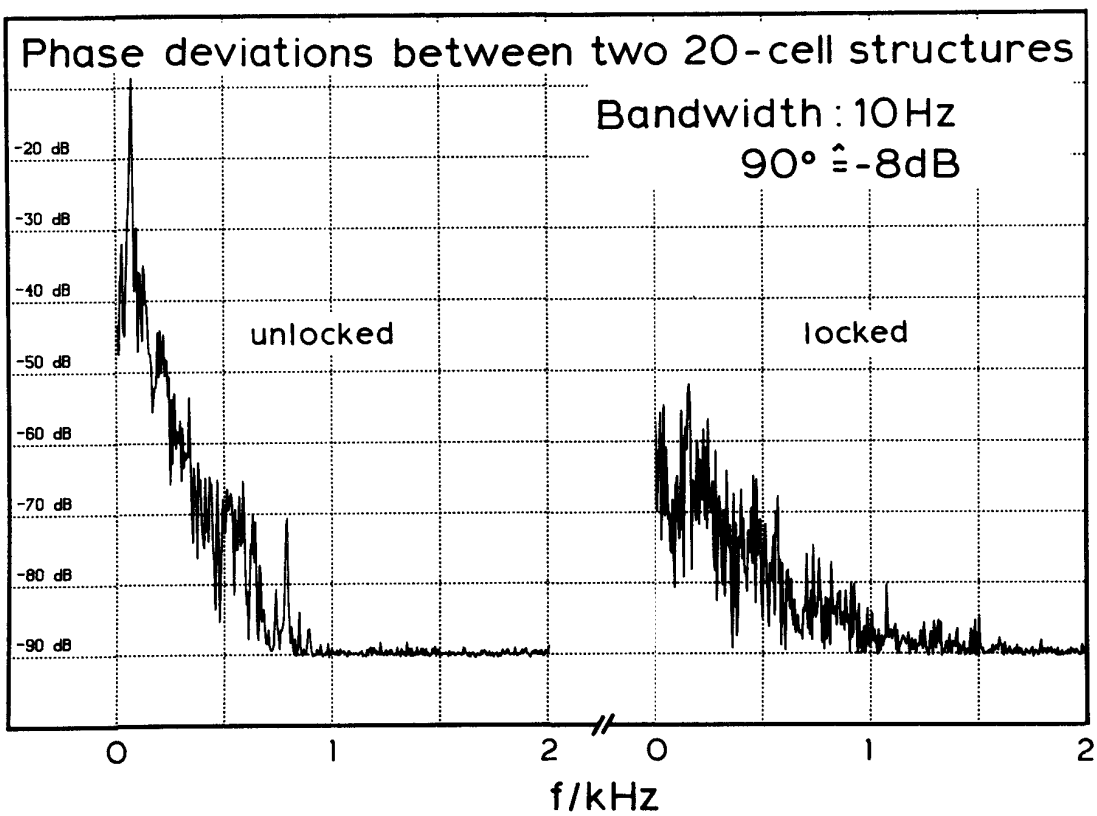

Fig. 5 Spectra of phase deviations between two twenty cell structures

The action of the phase control loop is demonstrated in Fig. 5 where the output signal of a double balanced mixer fed with the rf output signals from the two 20 cell structures is frequency analyzed. The left part of the figure shows the unlocked condition, when both structures are oscillating in self excited loops. The difference in frequency is 70 Hz showing up as a pronounced "carrier frequency" peak in the spectrum which can be used as a calibration for a 90 ^{o} phase deviation. The right part of Fig. 5 shows a frequency spectrum of the same signal when the two self excited loops are locked by the phase control circuit. All the remaining amplitudes in the phase deviation signal are at least 42 dB below the "carrier" peak of the left part, which means they are smaller than 0.5 ^{o}.

Phase locked operation of all three structures in the injector linac was achieved just a couple of weeks ago and results from beam tests are given in Sect. IV below.

The rf control circuit

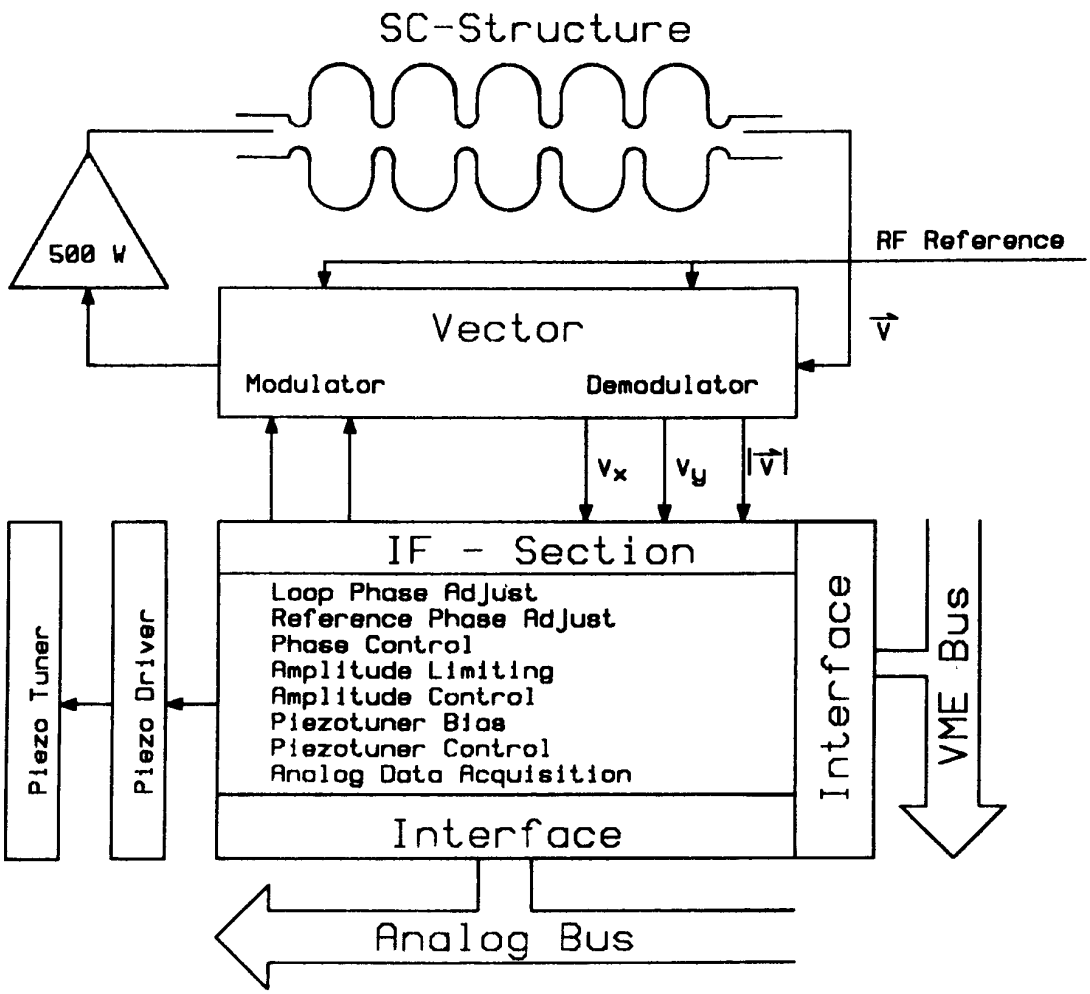

Fig. 6 Functional diagram of the rf circuit

In the rf and beam tests mentioned above the phase controlling element, a complex phasor modulator (CPM), had to be improvised using a power divider, a quadrature hybrid and two double balanced mixers as modulators since no CPM for 3 GHZ was commercially available. Therefore and since rf elements for 3 GHZ are much more expensive than at lower frequencies we decided for a final design of the rf control circuit very similar to the one described in ref. [4]. This design uses a minimum of rf components and performs all control operations in the IF section of the circuit. A functional block diagram of the rf circuit for one superconducting structure is shown in Fig. 6.

The 500 W klystron (top left of Fig. 6) drives the structure. A sample $\vec{V}$ of the field present in the structure is fed into a vector demodulator together with an rf reference signal. The output signals from the demodulator V_x and V_y which describe the signal $\vec{V}$ in the rotating coordinate system of the rf reference are taken to the IF section together with a signal proportional to the magnitude of $\vec{V}$ which is obtained by an additional rf amplitude detector diode. The two output signals from the IF section drive a vector modulator which generates the drive signal for the klystron from the rf reference and thus closes the self excited loop of the rf circuit.

All the functions performed in the IF section are listed in its box in Fig. 6. It contains the loop and reference phase shifters, feedback control for phase and amplitude, a limiter circuit necessary in a self excited loop and delivers a bias and feedback control signal for the piezoelectric fine tuner. A multiplexed ADC allows digital acquisition of input, output and error signals. The IF section is controlled by a 68000 microprocessor via VME Bus and the microprocessor is connected via a serial link to the remote LSI 11/73 described in Sect. III. Eight signals from the IF section can be switched to an analog bus and are available in the local control area as well as in the main control room for observation on an oscilloscope.

A more detailed block diagram of the circuit is shown in Fig. 7. All the rf elements are contained in the left part of the figure. The vector modulator (top) and demodulator (bottom) together with the amplitude detector diode have been incorporated into a single stripline board. The only external rf elements needed are the reference oscillator, a small 20 dBm amplifier to drive the klystron and the klystron itself. The right part of Fig. 7 contains the IF section. The two signals from the vector demodulator (referred to as V_x and V_y in Fig. 6) enter the circuit through variable gain buffer amplifiers and travel through the loop phase shifter which acts as a rotational matrix. The phase modulation circuit adds a signal in quadrature, the magnitude of which is determined by the phase control circuit. The final modulator stage is controlled by the limiter and amplitude control circuit to its right; the signal from the detector diode is delivering the information about the field strength in the cavity.

The signal for the phase control is derived from the input signals after passing through a reference phase shifter: it controls the phase modulator and after passing through a low pass filter it is added to the bias for the piezoelectric tuner. This way manual fine tuning (by changing the bias with the control signal disconnected) as well as automatic correction of slow frequency drifts is accomplished. For reasons of simplicity only four input lines to the ADC are shown and the connections to the analog bus as well as an out of lock detection circuit have been omitted.

At present a prototype of the rf board of the circuit is completed for testing, whereas the board of the IF section is still worked on.

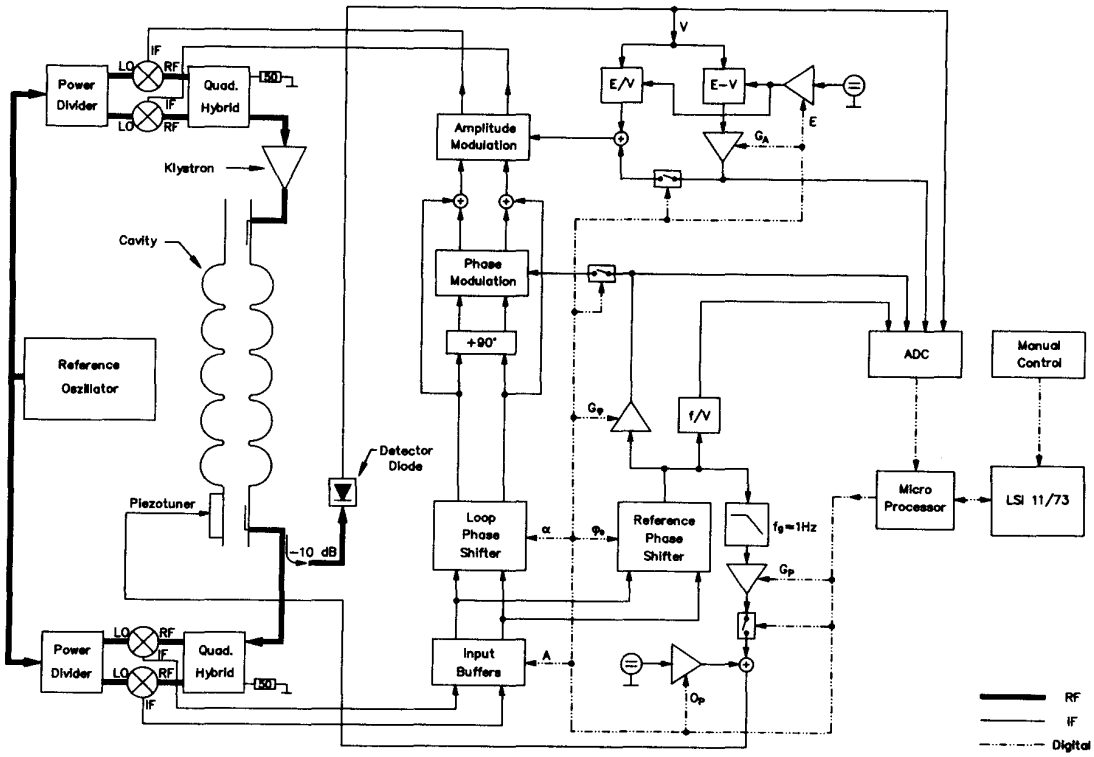

Fig. 7 **Block diagram of the rf control circuit**

IV. Injector Beam Tests

Late in August 87 a first beam accelerated by the capture section and two 20 cell structures was obtained. Information about its energy was obtained in two ways: (i) the beam was deflected by a 40^{0} bending magnet (part of the channeling radiation source setup) in the straight beamline behind the injector linac (see Fig. 1) and transported to a faraday cup. From the magnetic field of the deflection magnet an energy of about 6.7 MeV could be inferred. (ii) A more accurate result was obtained by using the bremsstrahlung facility at the end of the injection beamline and taking bremsstrahlung spectra at zero degrees with a NaJ detector.

Three such spectra are presented in Fig. 8 (please note the broken scale for the counts). The upmost spectrum results from a beam accelerated by all three structures and yields an endpoint energy of 6.8 MeV. The bump around 1.2 MeV results from a cobalt source positioned near the detector for calibration purposes. The spectrum in the center was taken using only the capture section and the first 20 cell structure, yielding an endpoint energy of 4.3 MeV. The spectrum in the lower left part of the figure with an endpoint energy of 1.2 MeV results from a beam accelerated by the capture section only (the cobalt source had been removed in this case).

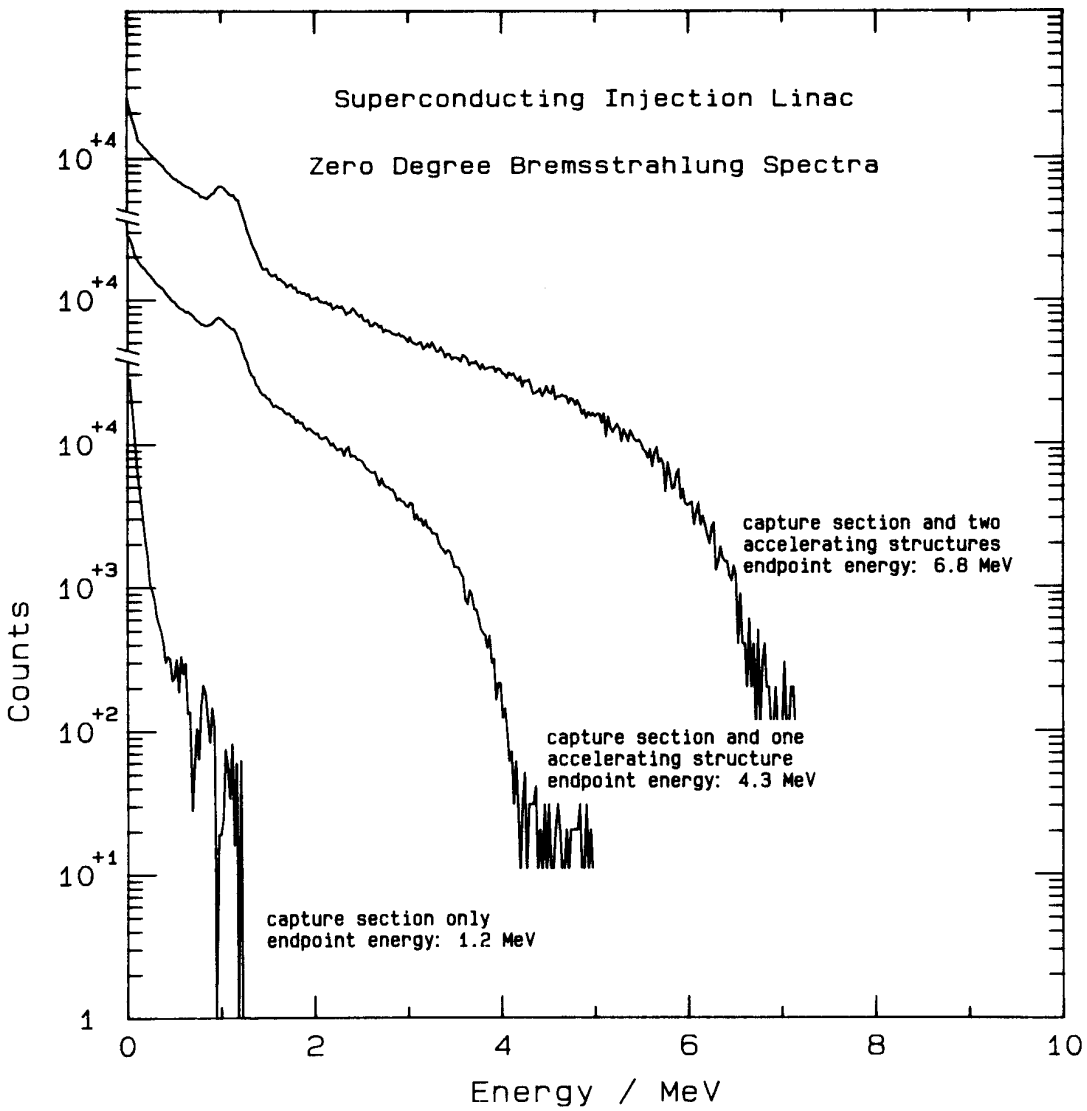

Fig. 8 Bremsstrahlung spectra obtained from a beam accelerated by 1, 2, and 3 superconducting structures

Taking into account the phase slip of the bunches in the $\beta = 1$ capture section as shown earlier [6] the beam energy of 1.2 MeV corresponds to an accelerating field of 6.0 MV/m. Similarly we obtain 3.2 MV/m and 2.5 MV/m for the first and second 20 cell structure respectively. These results are not only disappointing because of the low fields but also very interesting if one regards the history of the structures. The capture section and the second 20 cell structure are both fabricated from high purity material and yielded very high field strengths after their first preparation at Wuppertal of 12 MV/m and 7 MV/m respectively. Then they were mounted into their tuning frames at Wuppertal, transported to Darmstadt and mounted in the cryostat. In the meantime they had to be disassembled and remounted two times and apparently they suffered from this treatment. The first 20 cell structure, fabricated from the old low purity material never showed a field in excess of 3.3 MV/m but remained that way even though it was treated exactly like the other two struc-

tures. Therefore one of our next steps will be trying to improve the performance of the capture section and the second 20 cell structure by helium processing.

Up to now we hesitated to increase the beam current to i > 10 μA; we will first try to become a little more experienced in the operation of the injector by running it for several weeks.

V. Outlook

For the near future there are several goals to be reached. As already mentioned we will try to obtain higher fields in the injector linac by helium processing. The beam will be taken around the 180^{o} injection bend to the main linac side. After gaining some operation experience we will increase the current and try to perform a few experiments. In the meantime two other 20 cell structures will be mounted into another cryomodule and after the next warmup they will be installed as the first quarter of the main linac. Once the prototype boards for the rf control circuits have been tested the production for the twelve channels needed for the accelerator can start. So if we do not encounter unexpected severe problems we could have 5 structures in operation by the end of this year.

Then the main linac has to grow in steps of one cryomodule containing two 20 cell structures at a time. Since the installation of the two recirculations is almost finished as can be seen in Fig. 3 (only the cooling circuits for the dipole magnets are not operational yet) we look forward to the completion of the accelerator in 1988.

Acknowledgement

We are very much indebted to I. Ben - Zvi for his essential help during his visit in Darmstadt. The support from H. Lengeler and E. Haebel by fruitful discussions and help with equipment is gratefully acknowledged. We thank G. Sprouse for providing us with important informations and his encouragement. Without the help of U. Klein and H. Peiniger from Interatom with their equipment some important measurements could not have been performed. We are very grateful for the enormous help provided by the technical staff at the DALINAC and the mechanical and electronics workshops of both respective institutions.

References

[1] H.-D. Gräf, H. Miska, E. Spamer, O. Titze and Th. Walcher, Nucl. Instr. 153 (1978) 9.

[2] H.Heinrichs, U. Klein, G. Müller, H. Piel, D. Proch, W. Weingarten, H.Genz, H.-D. Gräf, T. Grundey, A.Richter, E. Spamer, Lecture Notes in Physics 108 (1979) 176.

[3] K. Alrutz - Ziemssen, H.-D. Gräf, V. Huck, K. D. Hummel, G. Kaster M. Knirsch, A. Richter, M. Schanz, S. Simrock, E. Spamer, O. Titze, Th. Grundey, H. Heinrichs, H. Piel, Proc. 1986 Lin. Acc. Conf , SLAC 303, Stanford, Cal. USA (1986)

[4] J. R. Delayen, G. J. Dick and J. E. Mercereau, IEEE Trans. Nucl. Sci. NS – 24, No. 3 (1977) 1759.

[5] I. Ben - Zvi, M. Birk, C. Broude, G. Gitliz, M. Sidi, J. S. Sokolowski and J. M. Brennan, Nucl. Instr. A 245 (1986) 1.

[6] T. Grundey, H. Heinrichs, U. Klein, G. Müller, G. Nissen, H. Piel, H. Genz, H.-D. Gräf, M. Janke, A. Richter, M. Schanz, E. Spamer and O. Titze, Nucl. Instr. 224 (1984) 5.